ACS Catalysis

Research Article

pubs.acs.org/acscatalysis

Hydrogen-Transfer Catalysis with Cp*Ir^{III} Complexes: The Influence of the Ancillary Ligands

Ulrich Hintermair,*[,†,§] Jesús Campos,[†] Timothy P. Brewster,[†,#] Lucas M. Pratt,[†] Nathan D. Schley,[†,‡] and Robert H. Crabtree*[,†]

[†]Department of Chemistry, Yale University, 225 Prospect Street, New Haven, Connecticut 06520, United States

[§]Centre for Sustainable Chemical Technologies, University of Bath, Claverton Down, Bath BA2 7AY, United Kingdom

Supporting Information

ABSTRACT: Fourteen Cp*Ir^{III} complexes, bearing various combinations of N- and C-spectator ligands, are assayed in hydrogen-transfer catalysis from isopropyl alcohol to acetophenone under various conditions to investigate ligand effects in this widely used reaction. The new cationic complexes bearing monodentate pyridine and N-heterocyclic carbene (NHC) ligands were characterized crystallographically and by variable-temperature nuclear magnetic resonance (VT-NMR). Control experiments and mercury poisoning tests showed that iridium(0) nanoparticles, although active in the reaction, are not responsible for the high activity observed for the most active precatalyst [Cp*Ir(IMe)$_2$Cl]BF$_4$ (**6**). For efficient catalysis, it was found necessary to have both NHCs in monodentate form; tying them together in a bis-NHC chelate ligand gave greatly reduced activity. The kinetics of the base-assisted reaction showed induction periods as well as deactivation processes, and H/D scrambling experiments cast some doubt on the classical monohydride mechanism.

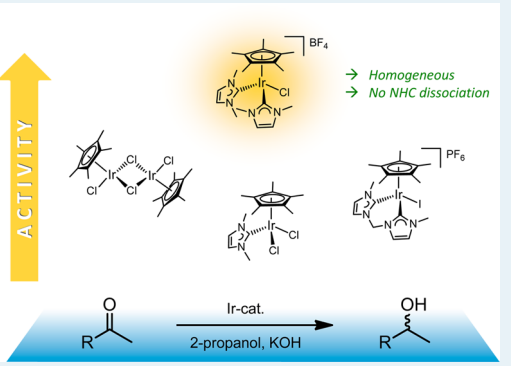

KEYWORDS: *transfer hydrogenation, Cp*Ir complexes, N-heterocyclic carbenes, homogeneous catalysis, kinetics, monohydride mechanism*

INTRODUCTION

Transfer hydrogenation is a useful reduction protocol increasing in popularity, in part because these reactions can be performed using a variety of liquid or solid hydrogen donors without the need for hydrogen gas.[1] Furthermore, the reversibility of the ionic H^+/H^- transfer[2] forms the basis for many useful C−C, C−O, and C−N bond-forming reactions via "borrowing-hydrogen" methodology.[3−6] The first catalytic systems mediating hydrogen transfer reported by Mitchell and Henbest[7−9] and Mestroni[10] were based on iridium compounds, and iridium catalysts are still among the most widely used today.[11] In the early 2000s, Ikariya and Noyori[12] and Fujita and Yamaguchi[13] introduced half-sandwich Cp*Ir complexes (including chiral versions[14−16]) as easily accessible and versatile precatalysts, which have quickly found wide use.[17] More recently, some Cp*Ir-NHC complexes (where NHC is N-heterocyclic carbene) have been shown to be particularly effective.[18−20] Several Cp*Ir precatalysts are currently commercially available, and the first examples are moving toward industrial application.[21]

The commonly accepted mechanism of Cp*Ir-catalyzed hydrogen transfer follows the "monohydride route", assuming full retention of all ancillary ligands.[22] Although this pathway represents a reasonable scenario in analogy with other transition-metal based catalysts, it fails to fully account for ligand effects in the Cp*Ir precursors,[23] partly because the kinetics are still rather poorly understood. Here, we present a systematic study of a small library of Cp*Ir complexes with nonfunctional[24] C- and N-donor spectator ligands in hydrogen-transfer catalysis to investigate ligand effects in this important transformation. In this paper, we focus on the effect of the ancillary ligands around the Cp*Ir fragment, while, in a future contribution, we will examine the role of the Cp* ligand. A highlight of the present work is the development of a new, highly active Cp*Ir precatalyst that may follow a different mechanism from that commonly assumed for this type of precursor.

RESULTS AND DISCUSSION

Complexes **1**−**14** (Figure 1) were designed as catalyst precursors to probe the influence of pyridines versus NHCs (**1** vs **2** vs **3**, **4** vs **5** vs **6**, **8** vs **10** vs **11**), chelating versus monodentate (**4** vs **11**, **5** vs **10**, **6** vs **8**), LL-type versus LX-type (**10** vs **13**, **11** vs **14**), and remote pH-switchable ligands (**10** vs **12**).

The reactivity switch of Ag-NHC complexes from mono-NHC transfer to bis-NHC transfer as a function of the coordination ability of the anion described previously for

Received: September 20, 2013
Revised: November 21, 2013
Published: November 26, 2013

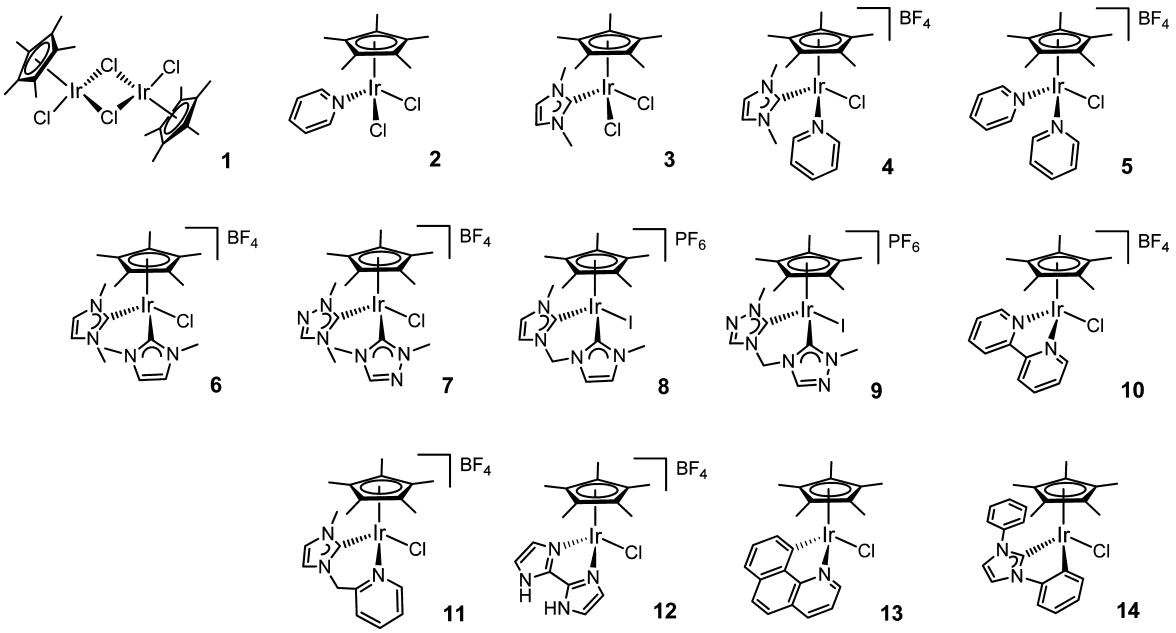

Figure 1. Cp^*Ir^{III} complexes evaluated in transfer hydrogenation catalysis.

Scheme 1. Single NHC Transfer (Left) versus Double NHC Transfer with Anion Metathesis (Right) at $[Cp^*IrCl_2]_2$, depending on the Ag-NHC Complex Used[a]

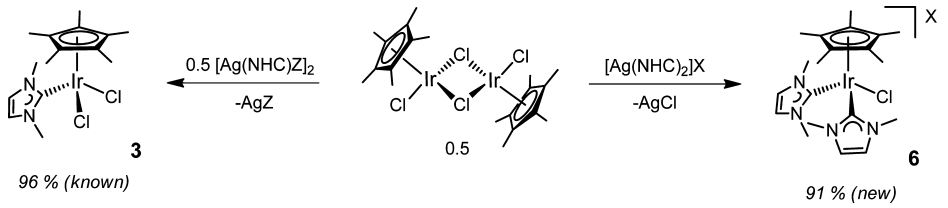

[a]Z = halide, X = weakly coordinating anion.

transmetalation reactions with Rh^I and Ir^I complexes,[25] was also found to apply to $[Cp^*IrCl_2]_2$ and allowed convenient access to mono- and bis-NHC complexes **3**, **6**, and **7**, respectively (see Scheme 1 and Figure 2). All other compounds were obtained via slight modifications of known procedures and isolated in good to excellent yields as air- and moisture-stable, crystalline solids after purification (see the Experimental Section).

Compounds **4**, **5**, **6**, **7**, **9**, and **12** have been characterized by single-crystal X-ray diffraction (Figure 2), while crystal structures of **3**,[26] **8**,[27] **10**,[28] **11**,[26] **13**,[29] and **14**[30] have been reported previously. In the solid state, all complexes have the expected piano-stool geometry without any unexpected features. As summarized in Table 1, ligand bite-angles and bond lengths are very similar in the chelating and monodentate cationic complexes.

In solution, both the pyridines and the minimally substituted IMe (1,3-dimethylimidazol-2-ylidene) and TMe (1,4-dimethyl-1,2,4-triazol-5-ylidene) ligands were found to rotate freely around the L–M axis on the NMR time scale at room temperature, even in the bis-ligated complexes **4**–**7**, indicating little steric hindrance. Variable-temperature ^1H nuclear magnetic resonance (VT-NMR) at 500 MHz in CD_2Cl_2 showed decoalescence of the IMe signals in **6** below 223 K, and decoalescence of the TMe in **7** below 233 K (see the Supporting Information). In the mixed py/IMe complex **4**, the IMe ligand peaks split below 248 K, while the pyridine ligand gave one set of sharp peaks down to 193 K (see the Supporting Information).

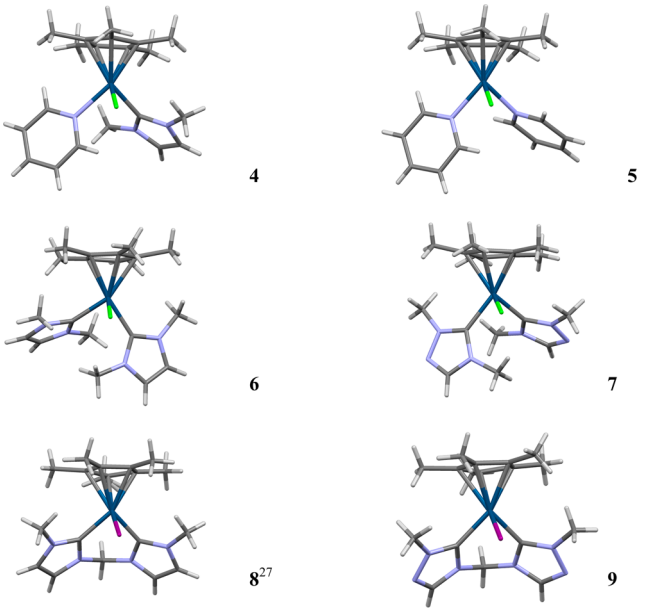

Figure 2. X-ray crystal structures of complexes **4**, **5**, **6**, **7**, **8**,[27] and **9** (counterions and solvent molecules omitted for clarity).

dx.doi.org/10.1021/cs400834q | ACS Catal. 2014, 4, 99–108

Table 1. Comparison of Selected Structural Data of Cp*Ir Complexes in the Solid State

complex	Ir−L distances	L−Ir−L angles
4	2.08 Å (C), 2.16 Å (N)	87.3°
5	2.16 Å	83.9°
6	2.06 Å	86.1°
7	2.05 Å	85.0°
8[27]	2.02 Å	86.4°
9	2.04 Å	85.0°
10[28]	2.10 Å	76.1°
11[26]	2.02 Å (C), 2.10 Å (N)	85.4°
12[31]	2.11 Å	75.4°
13[29]	2.06 Å (C), 2.10 Å (N)	78.8°
14[30]	2.00 Å (NHC), 2.05 Å (aryl)	77.6°

Freshly purified complexes **1**−**14** were evaluated for activity in the transfer hydrogenation of acetophenone at 1 mol % [Ir] loading after 3 h in refluxing ^{i}PrOH (~82 °C) under N_2 (Scheme 2). Reactions were run in the presence of 10 mol % KOH, 2 mol % $AgBF_4$, or without any additional promoter. Conversions were determined by ^{1}H NMR spectroscopy using 1,3,5-trimethoxybenzene as an internal standard.

Scheme 2. Transfer Hydrogenation of Acetophenone to *rac*-1-phenylethanol from Excess Isopropanol

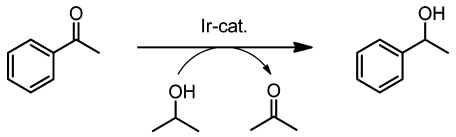

As can be seen from Figures 3−5, the conversion to product varied widely, depending on the conditions applied and

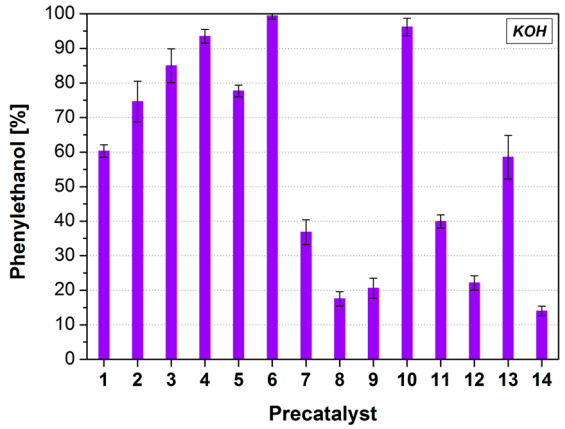

Figure 3. Activity of complexes **1**−**14** in the transfer hydrogenation of acetophenone (see Scheme 2). Reaction conditions: 2 mmol substrate, 1 mol % [Ir], 10 mol % KOH, 3 mL ^{i}PrOH, reflux, N_2, 3 h (^{1}H NMR analysis with 1,3,5-trimethoxybenzene as internal standard, triplicates).

precatalyst used. With the assistance of 10 mol % KOH, most precatalysts afforded significant conversion except complexes **8**, **9**, **12**, and **14**. Interestingly, the simple $[Cp^*IrCl_2]_2$ precursor **1** outperformed many of the more sophisticated Cp*Ir complexes, although **6** and **10** were clearly the most effective precatalysts under these conditions. Using Ag^+ as an activating agent instead of a base gave lower conversions and different trends in activity. Complexes **4** and **5**, bearing a labile pyridine

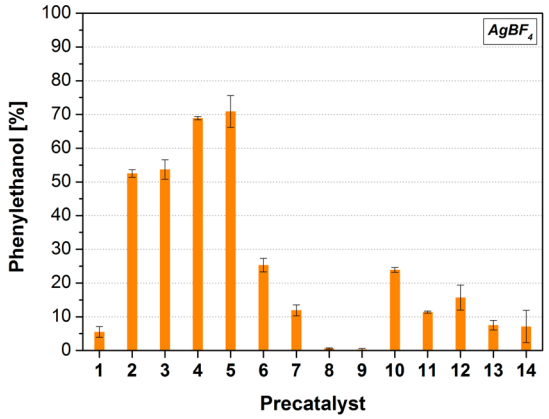

Figure 4. Activity of complexes **1**−**14** in the transfer hydrogenation of acetophenone (see Scheme 2). Reaction conditions: 2 mmol substrate, 1 mol % [Ir], 2 mol % $AgBF_4$, 3 mL ^{i}PrOH, reflux, N_2, 3 h (^{1}H NMR analysis with 1,3,5-trimethoxybenzene as internal standard, duplicates).

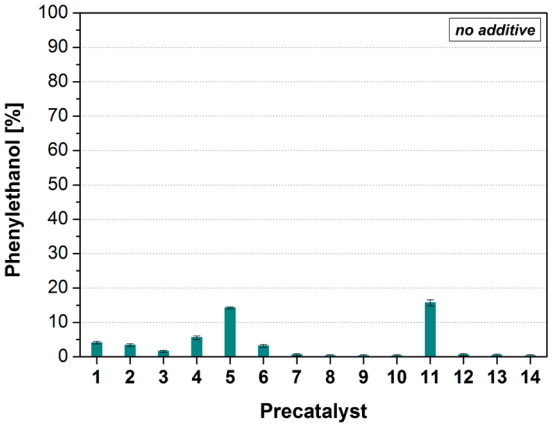

Figure 5. Activity of complexes **1**−**14** in the transfer hydrogenation of acetophenone (see Scheme 2). Reaction conditions: 2 mmol substrate, 1 mol % [Ir], 3 mL ^{i}PrOH, reflux, N_2, 3 h (^{1}H NMR analysis with 1,3,5-trimethoxybenzene as internal standard, duplicates).

base, gave the best results of ~70% conversion under these conditions. Attempted double activation with KOH and $AgBF_4$ gave virtually zero activity for all complexes (data not shown). A black precipitate formed in all of these reactions, suggesting in situ formation of Ag_2O, which effectively removes both Ag^+ and OH^- from the solution. Without any additive, activities were very low (<5%) for all precursors, except **5** and **11** (~15% conversion), as expected for precursors with nonfunctional spectator ligands.

The base-assisted reactions were found to be sensitive to both oxygen and moisture. No conversion was observed when performing the catalysis in air, and the addition of 50 μL of water (~140 equiv, with respect to [Ir]) under N_2 equally shut down all activity. However, the addition of activated 3 Å molecular sieves to the reaction did not improve performance either. In acidic aqueous media (10−100 equiv HOTf or $HClO_4$ in 1:1−10:1 ^{i}PrOH/H_2O), even the most active precursor **6** was completely inactivated, in contrast to aqueous hydrogen transfer reactions with Cp*Ir precatalysts using formate as the reductant, where optimum activity is typically observed in acidic media (pH ~2 for NH_4COOH, pH ~3 for NaCOOH).[32]

Because the base-assisted reactions were the most efficient, we examined the background reactivity of KOH alone under

dx.doi.org/10.1021/cs400834q | ACS Catal. 2014, 4, 99−108

our conditions. Transfer hydrogenations of aldehydes and ketones are known to be slowly catalyzed by simple alkali metal bases,[33−35] and even alcohol alkylations can be achieved with base only.[36] Following activity over time showed that ∼16% phenylethanol was produced by 10 mol % KOH after 3 h at 80 °C (Figure 6), indicating that complexes **8**, **9**, **12**, **14** had

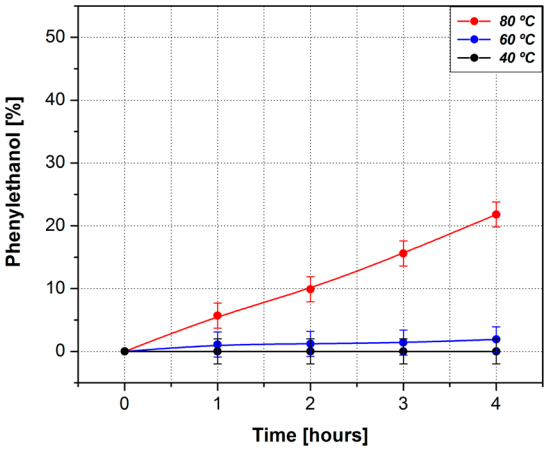

Figure 6. Background activity of KOH (10 mol %, semiconductor grade) in the transfer hydrogenation of acetophenone at different temperatures (2 mmol substrate, 3 mL ^{i}PrOH, N_2; ^{1}H NMR analysis with 1,3,5-trimethoxybenzene as internal standard; lines drawn to guide the eye).

effectively afforded zero activity (Figure 3). Lowering the temperature to 60 °C gave much lower base-catalyzed activity of only ∼2% after 4 h, and at 40 °C no product could be observed by ^{1}H NMR even after 12 h.

Next, some simple iridium compounds, including heterogeneous forms, were evaluated in the reaction to test for potential contributions from decomposition products of the Cp*Ir precursors (Table 2). Numerous heterogeneous catalysts,[37]

Table 2. Activity of Various Iridium Compounds in the Transfer Hydrogenation of Acetophenone (see Scheme 2)[a]

precatalyst	with KOH	no additive
$IrCl_3·3H_2O$	81% ± 2%	7% ± 1%
IrO_2 (powder)[b]	21% ± 3%	0%
Ir/C (0.5 wt %)[b]	29% ± 11%	0%
2−3 nm Ir^0 NPs[48]	94% ± 6%	4% ± 1%

[a]2 mmol substrate, 1 mol% [Ir], 3 mL ^{i}PrOH, reflux, N_2, 3 h (^{1}H NMR analysis with 1,3,5-trimethoxybenzene as internal standard, duplicates). [b]Dried at 80 °C in vacuo for at least 3 h prior to use.

including IrO_2,[38] and various metal nanoparticles (NPs) are known to catalyze transfer hydrogenations quite efficiently,[39−44] and for some related iron and ruthenium complexes metallic NPs have recently been shown to contribute to catalytic activity.[45,46] In situ deligation of molecular precursors to give heterogeneous material as the true active species is a persistent ambiguity in homogeneous catalysis often responsible for misleading ligand effects.[47]

As expected from the early work of Mitchell and Henbest,[9] $IrCl_3$ hydrate afforded good activity with >80% conversion in 3 h, surpassing many of the Cp*Ir precursors under identical conditions (cf. Figure 3). While IrO_2 and iridium on carbon barely added to the background activity of KOH, iridium(0) nanoparticles synthesized in situ[48] prior to catalysis were highly active in the presence of a base (see Table 2). These findings might at first appear indicative of Ir NPs being the true catalyst in all cases, with the activity trends merely reflecting the ease of reductive in situ decomposition. Therefore, we performed reactions with Ir NPs, $IrCl_3$, and **6** in the presence of excess Hg to selectively poison heterogeneous forms of metallic iridium[49] (see Table 3). While the preformed NPs were effectively

Table 3. Mercury Poisoning Test of Different Iridium Precatalysts in the Transfer Hydrogenation of Acetophenone (see Scheme 2)[a]

precatalyst	no Hg	with Hg
6	99 ± 1%	98 ± 1%
$IrCl_3·3H_2O$	39 ± 1%	37 ± 1%
2−3 nm Ir NPs[b]	64 ± 1%	5 ± 1%

[a]2 mmol substrate, 1 mol% [Ir], 10 mol% KOH, 3 mL ^{i}PrOH, 60 °C, N_2, 3 h (^{1}H NMR analysis with 1,3,5-trimethoxybenzene as internal standard). [b]Data taken from ref 48.

deactivated by mercury, both $IrCl_3$ and **6** displayed virtually unperturbed activity in its presence, strongly suggesting genuine solution-phase catalysis in the case of the molecular precursors.[50]

After having subtracted the background reactivity of the base and provided evidence against in situ decomposition into heterogeneous catalysts, we can discuss the activities of the most active precursors $IrCl_3$, **1**−**6**, and **10** in comparison with the less active ones. Clearly, both IMe and pyridine are good supporting ligands for Cp*Ir transfer hydrogenation catalysts, but no obvious trends regarding ligand denticity, sterics, or electronics are apparent from this dataset collected under strictly comparable conditions. For example, linking the two pyridines in **5** to give a bipy ligand in **10** slightly increases catalyst activity, whereas the same strategy has an opposite effect in the case of two IMe in **6** versus **8** or one IMe and one pyridine as in **4** versus **11**. Also, going from IMe to TMe, a subtle change in electronics[51] dramatically decreases catalyst activity in **7** as compared to **6**. Further decreasing the ligand donor power by moving to **5** and **10** gave intermediate activity. Only one discernible trend emerged: assuming **12** was deprotonated under reaction conditions, one could conclude that LX-type chelate ligands are inferior to LL-type combinations.

In view of the surprisingly high performance of the unlinked bis-NHC complex **6**, we monitored the reaction progress of $IrCl_3$, **1**, **3**, and **6** via in situ ^{1}H NMR at lower temperature to compare the effects of introduction of the Cp* and IMe ligands (Figure 7). At 60 °C, $IrCl_3$ was barely active (20% conversion after 3 h), but introducing the Cp* ligand (**1**) caused a marked increase in activity (70% conversion after 3 h). Further introduction of one IMe ligand to the Cp*Ir fragment (**3**) decreased activity again, whereas introduction of the second IMe ligand (**6**) boosted catalyst activity to afford full conversion in less than 2 h. This striking difference in performance of **3** and **6** demonstrates that both monodentate IMe ligands in **6** are needed for efficient transfer hydrogenation catalysis and suggests their retention during turnover.

We then further explored the transfer hydrogenation scope of **6**. At 1 mol % loading, full conversion of various aromatic and aliphatic ketones was achieved within 3 h at 60 °C (Table 4). *α*,*β*-unsaturated ketones (entries 11 and 12) were found to be completely reduced to the saturated alcohols with >90%

dx.doi.org/10.1021/cs400834q | ACS Catal. 2014, 4, 99−108

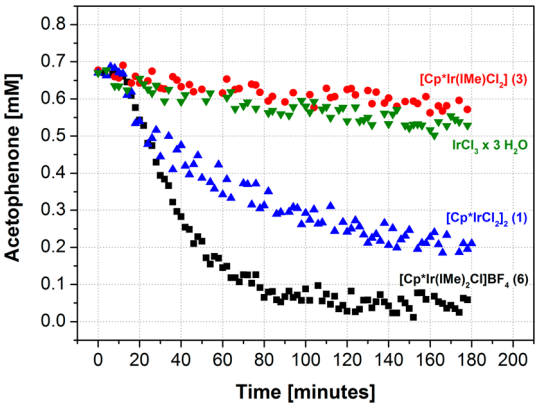

Figure 7. Activity of different iridium precatalysts in the transfer hydrogenation of acetophenone (Scheme 2). Reaction conditions: 0.67 mmol substrate, 1 mol% [Ir], 10 mol% KOH, 1 mL ^{i}PrOH, 60 °C, N_2 (in situ ^{1}H NMR analysis with 1,3,5-trimethoxybenzene as internal standard).

conversion. In refluxing isopropyl alcohol, **6** still afforded activity at 0.01 mol % loading to reach turnover numbers beyond 3000 after 6 h (entries 3 and 6).

In search of a rationale for the observed ligand effects, the kinetics of the acetophenone reduction with **6** were investigated. Variation of the KOH loading with 1 mol % [Ir] at 60 °C showed that the rate was clearly base-dependent with slower turnover at lower base loading (Figure 8); however, because of the sigmoidal shape of the reaction profile, kinetic analysis with respect to the order in base could not be

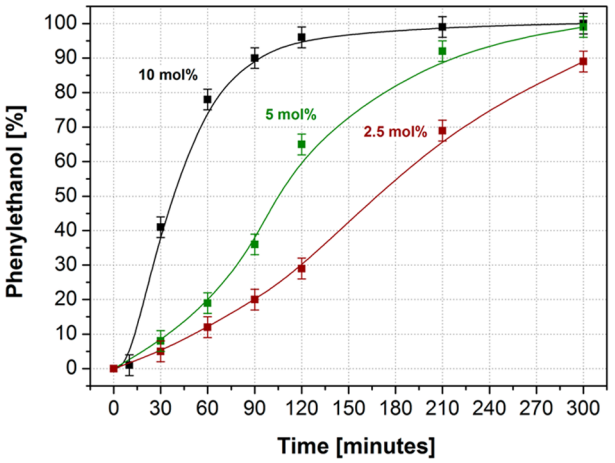

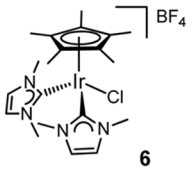

6

Figure 8. Activity of **6** in the transfer hydrogenation of acetophenone (see Scheme 2) at various loadings of KOH. Reaction conditions: 2 mmol substrate, 1 mol % [Ir], 3 mL ^{i}PrOH, 60 °C, N_2 (^{1}H NMR analysis with 1,3,5-trimethoxybenzene as internal standard; lines drawn to guide the eye).

performed. As previously observed (Figure 7), a nonproductive lag phase of several minutes was always observed, which was

Table 4. Performance of Precatalyst 6 at Different Loadings in the Transfer Hydrogenation of Various Substrates from ^{i}PrOH[a]

entry	*mol% of 6*	*substrate*	*conversion*	*TON*
1[b]	1.0		99 ± 1 %	99 ± 1
2	0.1		99 ± 1 %	990 ± 10
3[c]	0.01		31 ± 1 %	3100 ± 100
4[b]	1.0	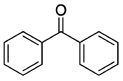	99 ± 1 %	99 ± 1
5	0.1		99 ± 1 %	990 ± 10
6[c]	0.01		23 ± 1 %	2300 ± 100
7[b]	1.0	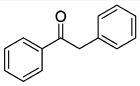	99 ± 1 %	99 ± 1
8[b]	1.0	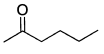	99 ± 1 %	99 ± 1
9[b]	1.0		99 ± 1 %	99 ± 1
10[b]	1.0		99 ± 1 %	99 ± 1
11[b]	1.0		94 ± 1 %[d]	94 ± 1 (×2)[d]
12[b]	1.0		95 ± 1 %[d]	95 ± 1 (×2)[d]

[a]2 mmol substrate, 10 mol% KOH, 3 mL ^{i}PrOH, reflux, N_2, 3 h (^{1}H NMR analysis with 1,3,5-trimethoxybenzene as internal standard). [b]At 60 °C. [c]After 6 h. [d]Complete reduction to saturated alcohol.

dx.doi.org/10.1021/cs400834q | *ACS Catal.* 2014, 4, 99−108

virtually unaffected by the amount of KOH present. Nevertheless, high conversions were still reached after longer reaction times at lower base loading, which may be beneficial for the reduction of sensitive substrates where time is less important.

Varying the concentration of **6** at a fixed KOH loading of 10 mol % showed that both the length of the nonproductive lag phase and the rate of acetophenone reduction were strongly dependent on the iridium concentration (Figure 9).

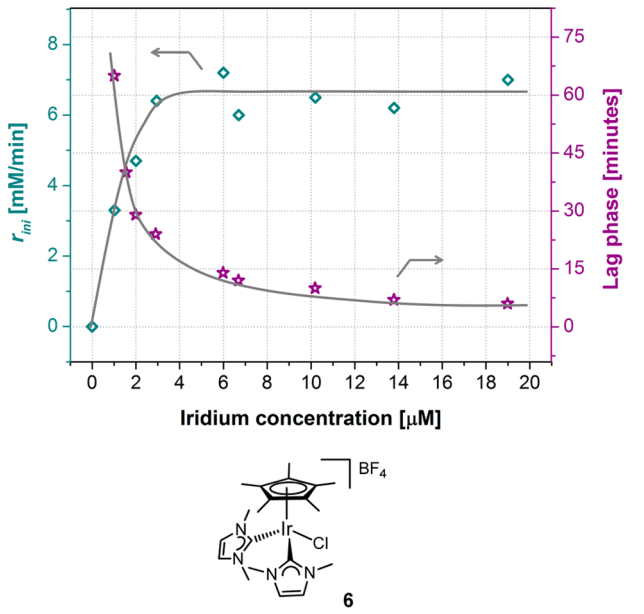

Figure 9. Lag phases (stars, right axis) and approximate initial rates (diamonds, left axis) of the transfer hydrogenation of acetophenone (see Scheme 2) by **6** at various catalyst loadings. Reaction conditions: 0.67 mmol substrate, 10 mol % KOH, 1 mL ^{i}PrOH, 60 °C, N_2 (in situ ^{1}H NMR analysis with 1,3,5-trimethoxybenzene as internal standard; lines drawn to guide the eye).

The lag phase dependence on [Ir] cleanly followed second-order kinetics with an apparent rate constant of k_{obs} = 61 μM^{-1} min^{-1}, suggesting a precatalytic activation step involving two iridium centers (Figure 10). The rates at the onset of catalysis, which could be estimated at 10 mol % base (cf. Figure 8), showed two distinct kinetic regimes. Below ~4 μM [Ir], the initial rate of acetophenone reduction after the lag phase was clearly dependent on [Ir], whereas at higher concentrations an apparent zero-order regime prevailed. Limiting base/Ir ratios were ruled out by testing catalysis at 6.7 μM **6** (= 1 mol %) with 25 mol % base instead of the usual 10 mol % (as in Figures 7 and 8), which gave no further increase in the rate of acetophenone reduction. Therefore, we suspect an [Ir]-dependent catalyst deactivation process after preactivation to be responsible for the apparent rate saturation above ~4 μM [Ir].[52] With such complex kinetics, it is not surprising that our understanding of ligand effects in Cp*Ir precatalysts for these transformations is still so limited, despite their extensive use.

The commonly accepted mechanism of base-assisted transfer hydrogenations from isopropyl alcohol with Cp*Ir complexes follows the so-called "monohydride" route, in which the base shuttles the protic hydrogens between the alkoxides and the iridium catalyst delivers the hydrides from the carbinol to the carbonyl carbons (see Scheme 3).[23]

Accordingly, Cp*Ir-monohydride complexes are considered key intermediates in these reactions.[18,23] We thus synthesized

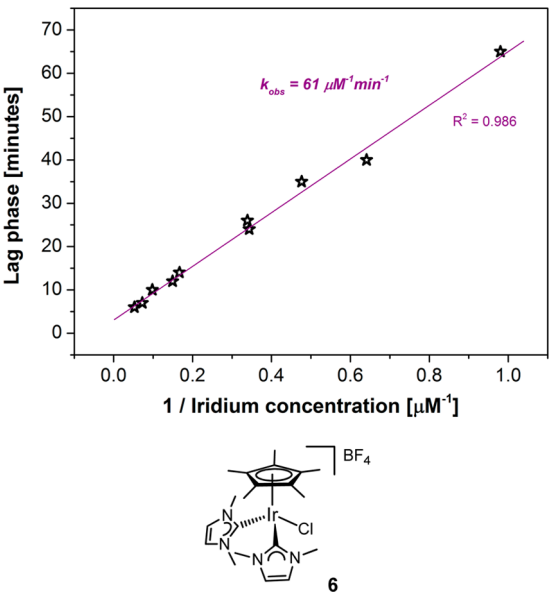

Figure 10. Second-order dependence of the duration of nonproductive lag phases in the transfer hydrogenation of acetophenone (see Scheme 2) by **6** on iridium concentration. Reaction conditions: 0.67 mmol substrate, 10 mol % KOH, 1 mL ^{i}PrOH, 60 °C, N_2 (in situ ^{1}H NMR analysis with 1,3,5-trimethoxybenzene as an internal standard).

Scheme 3. Commonly Accepted Hydrogen Delivery Scheme in the Monohydride Mechanism of Base-Assisted Transfer Hydrogenation Catalysis[23]

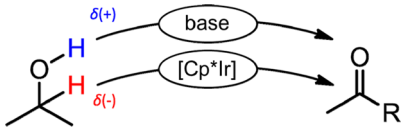

the corresponding monohydride complex of **6** by reaction with sodium borohydride, which gave the desired compound **6-H** as a colorless solid in high yield (see Scheme 4). The complex was found to be air and moisture stable and inert toward reductive elimination of $HIMe^+$ or halide exchange with chlorinated solvents at ambient temperature.

Scheme 4. Synthesis of Monohydride Complex 6-H (see Experimental Section for Details)

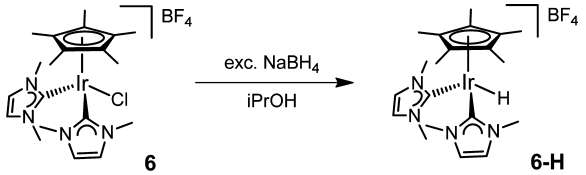

The ^{1}H NMR resonance of the terminal hydride in **6-H** at −16.24 ppm (in CD_2Cl_2) lies in the expected range, by comparison with similar complexes reported previously.[53−56] Using the same reaction protocol with complex **7**, only traces of the putative hydride **7-H** could be detected by ^{1}H NMR at −15.74 ppm in the crude reaction mixture and no stable product could be isolated. Complex **8**, however, successfully yielded the stable monohydride derivative **8-H** (−15.98 ppm)[27] after silver-assisted iodide abstraction (see the Experimental Section). Both **6-H** and **8-H** proved active in base-assisted transfer hydrogenation of acetophenone (Table 5), in contrast

dx.doi.org/10.1021/cs400834q | ACS Catal. 2014, 4, 99−108

Table 5. Comparison of Halide and Monohydride Complexes in the Transfer Hydrogenation of Acetophenone (see Scheme 2)[a]

precatalyst	conditions	conversion
6(Cl)	60 °C, 1 h	78% ± 1%
6-H	60 °C, 1 h	56% ± 1%
8(I)	reflux, 3 h	18% ± 2%
8(Cl)	reflux, 3 h	43% ± 1%
8-H	reflux, 3 h	7% ± 1%

[a]2 mmol substrate, 1 mol% [Ir], 10 mol% KOH, 3 mL ^{i}PrOH, N_2, (^{1}H NMR analysis with 1,3,5-trimethoxybenzene as internal standard).

to [Cp*Ir(NHC)$(H)_2$] (−16.9 ppm) and [Cp*Ir(NHC)$(\mu$-H)$]_2^{+2}$ (−17.4 ppm) complexes, which have been reported to be inactive and thus suspected relevant to catalyst deactivation pathways.[18] The inner-sphere chloride version **8**(Cl) of the iodide complex **8** was also prepared[27] for direct comparison with the chloride complex **6** and their corresponding hydrides. As can be seen from Table 5, the more strongly binding iodide had only a small inhibiting effect on activity in transfer hydrogenation catalysis. Although this simple activity comparison of halide versus monohydride complexes in the cases of **6** and **8** did not allow us to comment on their role in the catalytic cycle, it is worth mentioning that the monohydrides **10-H** (−11.80 ppm)[57] and **13-H** (−14.98 ppm)[58] are also known to be stable but only **10-H** has been reported to be active in transfer hydrogenation catalysis.[57] Bäckvall's test for monohydride pathways was then applied by following acetophenone reduction from 99% $(CD_3)_2$CD−OH by ^{1}H NMR using **6** and **6-H** to quantify the degree of H/D scrambling during hydrogen transfer (see Scheme 5).[22]

At 1 mol% [Ir] with 10 mol% KOH at 60 °C, the chloride complex **6** incorporated 75% D at the carbinol of phenylethanol, whereas for the hydride **6-H** 95% D incorporation at the same position were seen by in situ ^{1}H NMR. In both cases, the levels of product deuteration remained constant throughout the reaction up to 90% conversion as quantified against 1,3,5-trimethoxybenzene as internal standard (see Experimental Section for details). Thus, while **6-H** gave products consistent with the classic monohydride route, **6** gave an inconclusive result as to the number of metal hydrides involved, suggesting that **6-H** may not be the only possible hydride intermediate in catalysis with **6**.

CONCLUSION

We have synthesized and characterized several new Cp*Ir complexes bearing combinations of pyridine and NHC ligands, and we have compared their activity in transfer hydrogenation catalysis to structurally related literature compounds under various conditions. Contributions from the base and potential heterogeneous forms of iridium have been examined separately, and mercury poisoning experiments showed the Cp*Ir systems to be homogeneous. Complex **6** bearing two monodentate IMe ligands emerged as the most active precatalyst for the reduction of acetophenone from isopropyl alcohol in the presence of KOH, surprisingly superior to its chelating bis-NHC congener. At lower temperatures of 60 °C, **6** reduces a variety of ketone substrates with full conversion within 2 h, reaching turnover numbers (TONs) of >3000 at 0.01 mol % loading. Reaction progress monitoring in comparison with the mono-NHC complex **3** showed that both NHCs are needed for efficient catalysis. The kinetics of the catalysis with **6** were complex, showing a bimolecular activation period followed by base-dependent hydrogen-transfer catalysis with an apparent rate saturation at [Ir] concentrations of >4 μM. A stable monohydride derivative of **6** has been synthesized which is active in the reaction, but H/D scrambling data suggest that it may not be the only intermediate in the catalytic cycle. Although the mechanistic reason for the superiority of **6** and the role of the monohydride in catalysis remain to be examined further in a following report, the present work provides important insight into this basic transformation and sheds some light on ligand effects in these widely used Cp*Ir precatalysts.

EXPERIMENTAL SECTION

General. Organic solvents were purified by passing over activated alumina with dry N_2. All chemicals were purchased from major commercial suppliers and used as received. Syntheses were performed under an inert atmosphere of dry N_2 using standard Schlenk techniques. NMR spectra were recorded on either 400 or 500 MHz Bruker Avance spectrometers and referenced to residual protio-solvent signals. The chemical shift δ is reported in units of parts per million (ppm). Mass spectroscopy (MS) analyses were performed by the Mass Spectrometry and Proteomics Resource of the W.M. Keck Foundation Biotechnology Resource Laboratory at Yale University. [1,3-dimethylimidazolium]BF_4 and [1,4-dimethyl-1,2,4-triazolium]BF_4,[60] [Cp*$IrCl_2]_2$ (**1**),[61] [Cp*Ir(IMe)Cl_2] (**3**),[26] [Cp*Ir(bis-IMe)I]PF_6 (**8**),[27] [Cp*Ir(bis-TMe)I]PF_6 (**9**),[62] [Cp*Ir(bipy)Cl]BF_4 (**10**),[28] *rac*-[Cp*Ir(py-IMe)Cl]BF_4 (**11**),[26] [Cp*Ir(biim)Cl]BF_4 (**12**),[31] *rac*-[Cp*Ir(bequi)Cl] (**13**),[29] and *rac*-[Cp*Ir(phe-IPh)Cl] (**14**)[30] were synthesized via slightly modified literature procedures. Single crystals suitable for X-ray crystallography were obtained by diffusion of Et_2O into concentrated CH_2Cl_2 solutions at room temperature. Details of the X-ray diffraction (XRD) experiments can be found in the Supporting Information.

*[(η^5-Pentamethylcyclopentadienyl)Ir^{III}(κN-pyridine)Cl_2] (**2**).* [Cp*$IrCl_2]_2$ (120 mg, 0.15 mmol) was dissolved in CH_2Cl_2 (10 mL) and pyridine (24 mg, 0.3 mmol) added, causing an immediate color change from orange to yellow. After stirring at room temperature for 15 min, the solvent was evaporated under reduced pressure, yielding a yellow-orange powder that did not change color upon

Scheme 5. Bäckvall's H/D Scrambling Test To Probe the Number of Hydrides in the Active Species of Transfer Hydrogenation (cf. Scheme 3)[a]

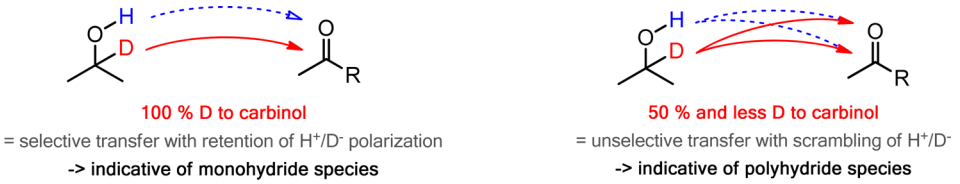

[a]Note that kinetic isotope effects may lead to >50% D transfer to the carbinol in the polyhydride mechanism, but would not affect the selectivity of the monohydride mechanism.[59]

dx.doi.org/10.1021/cs400834q | ACS Catal. 2014, 4, 99−108

drying in vacuo. Yield = 140 mg (98%). ^{1}H NMR (400 MHz, CD_2Cl_2): δ = 8.92 (dd, J = 6.5 Hz, J = 1.6 Hz, 2H, *o*-C*H*^{py}), 7.77 (tt, J = 7.7 Hz, J = 1.6 Hz, 1H, *p*-C*H*^{py}), 7.37 (ddd, J = 7.7 Hz, J = 6.5 Hz, J = 1.6 Hz, 2H, *m*-C*H*^{py}), 1.49 (s, 15H, $C_5(CH_3)_5$). ^{13}C{^{1}H}-NMR (100 MHz, CD_2Cl_2): δ = 153.7 (s, *o*-CH^{py}), 138.3 (s, *p*-CH^{py}), 125.9 (s, *m*-CH^{py}), 86.1 (s, $C_5(CH_3)_5$), 8.6 (s, $C_5(CH_3)_5$). ESI(+)MS calcd for $C_{15}H_{20}ClIrN^+$ (**2**-Cl): 440.089, 442.091. Found: m/z = 440.318, 442.313.

*rac-[(η^5-Pentamethylcyclopentadienyl)Ir^{III}(κC-1,3-dimethylimidazol-2-ylidene)(κN-pyridine)Cl]BF$_4$ (**4**).* [Cp*Ir(IMe)Cl$_2$] (**3**, 99 mg, 0.2 mmol) was dissolved in CH_2Cl_2 (10 mL) and pyridine (19 mg, 0.24 mmol) added. Upon the addition of $AgBF_4$ (39 mg, 0.2 mmol) in MeOH (1 mL), the mixture turned bright yellow with immediate precipitation of a colorless solid. After stirring at room temperature for 1 h, the solid was filtered off, discarded, and the clear solution dried in vacuo to leave a yellow solid. Recrystallization from acetone/Et_2O gave yellow microcrystals. Yield = 106 mg (85%). ^{1}H NMR (400 MHz, CD_2Cl_2): δ = 8.46 (d, J = 5.3 Hz, 2H, *o*-C*H*^{py}), 7.93 (t, J = 7.4 Hz, 1H, *p*-C*H*^{py}), 7.40 (t, J = 6.7 Hz, 2H, *m*-C*H*^{py}), 7.13 (s, 2H, NC*H*C*H*N), 3.51 (bs, 6H, NCH_3), 1.66 (s, 15H, $C_5(CH_3)_5$). ^{13}C{^{1}H}-NMR (100 MHz, CD_2Cl_2): δ = 155.0 (s, *o*-CH^{py}), 154.4 (s, NCN), 139.2 (s, *p*-CH^{py}), 127.3 (s, *m*-CH^{py}), 125.0 (s, NCHCHN), 91.9 (s, $C_5(CH_3)_5$), 38.2 (s, NCH_3), 9.5 (s, $C_5(CH_3)_5$). ESI(+)MS calcd for $C_{15}H_{23}ClIrN_2^+$ (**4**-BF$_4$-pyridine): 457.115, 459.117. Found: m/z = 457.351, 459.351. Crystal data [CCDC No. 961097]: $C_{20}H_{28}BClF_4IrN_3$ (**4**), M = 624.941, monoclinic, $P2_1/c$, a = 8.9512(10) Å, b = 24.437(3) Å, c = 10.4956(11) Å, β = 95.799(7)°, V = 2284.1(4) Å^3, Z = 4, d_{calc} = 1.817 g/cm^3, T = 223 K, 21642 reflections collected, 5195 independent reflections (R_{int} = 0.0747), final R_1 = 0.0490, final wR_2 = 0.0567, goodness of fit (GOF) = 1.066. [Note: CCDC stands for Cambridge Crystallographic Data Centre.]

*[(η^5-Pentamethylcyclopentadienyl)Ir^{III}bis-(κN-pyridine)Cl]BF$_4$ (**5**).* [Cp*IrCl$_2$]$_2$ (80 mg, 0.1 mmol) was dissolved in CH_2Cl_2 (5 mL) and pyridine (32 mg, 0.4 mmol) added, causing an immediate color change from orange to yellow. Upon the addition of $AgBF_4$ (39 mg, 0.2 mmol) in methanol (1 mL), a colorless solid precipitated instantly. After stirring at room temperature for 15 min, the solid was filtered off, discarded, and the clear solution dried in vacuo, leaving a yellow solid. Recrystallization from CH_2Cl_2/Et_2O gave bright yellow microcrystals. Yield = 108 mg (89%). ^{1}H NMR (400 MHz, CD_2Cl_2): δ = 8.95 (d, J = 5.1 Hz, 4H, *o*-C*H*^{py}), 7.91 (t, J = 7.6 Hz, 2H, *p*-C*H*^{py}), 7.54 (t, J = 7.0 Hz, 4H, *m*-C*H*^{py}), 1.49 (s, 15H, $C_5(CH_3)_5$). ^{13}C{^{1}H}-NMR (100 MHz, CD_2Cl_2): δ = 153.3 (s, *o*-CH^{py}), 139.9 (s, *p*-CH^{py}), 127.5 (s, *m*-CH^{py}), 89.0 (s, $C_5(CH_3)_5$), 8.6 (s, $C_5(CH_3)_5$). ESI(+)MS calcd for $C_{15}H_{20}ClIrN^+$ (**5**-BF$_4$-pyridine): 440.089, 442.091. Found: m/z = 440.081, 442.082. Crystal data [CCDC No. 961098]: $C_{20}H_{25}BClF_4IrN_2$ (**5**), M = 607.910, monoclinic, $P2_1/c$, a = 9.2867(17) Å, b = 14.334(3) Å, c = 16.829(3) Å, β = 90.266(5)°, V = 2240.1(7) Å^3, Z = 4, d_{calc} = 1.802 g/cm^3, T = 223 K, 14993 reflections collected, 4952 independent reflections (R_{int} = 0.0374), final R_1 = 0.0336, final wR_2 = 0.0661, GOF = 1.083.

*[(η^5-Pentamethylcyclopentadienyl)Ir^{III}bis-(κC-1,3-dimethylimidazol-2-ylidene)Cl]BF$_4$ (**6**).* [Ag(IMe)$_2$]BF$_4$ was prepared as a colorless crystalline solid from [1,3-dimethylimidazolium]BF$_4$, NaOH, and Ag_2O as described previously.[25] [Cp*IrCl$_2$]$_2$ (159 mg, 0.2 mmol) and [Ag(IMe)$_2$]BF$_4$ (155 mg, 0.4 mmol) were dissolved in dry CH_2Cl_2 (10 mL), and the resulting orange suspension was stirred for 1 h at room temperature. The colorless precipitate was filtered off, the solution concentrated to ~4 mL under reduced pressure, and filtered again through a 0.2 μm pore size Teflon filter. Addition of Et_2O (15 mL) caused precipitation of a yellow-orange powder, which was collected and dried in vacuo. Yield = 234 mg (91%). ^{1}H NMR (400 MHz, CD_2Cl_2): δ = 7.08 (s, 4H, NC*H*C*H*N), 3.44 (s, 12H, NCH_3), 1.64 (s, 15H, $C_5(CH_3)_5$). ^{13}C{^{1}H}-NMR (100 MHz, CD_2Cl_2): δ = 147.5 (s, NCN), 124.4 (s, NCHCHN), 96.1 (s, $C_5(CH_3)_5$), 38.6 (s, NCH_3), 10.6 (s, $C_5(CH_3)_5$). ESI(+)MS calcd for $C_{20}H_{31}ClIrN_4^+$ (**6**-BF$_4$): 553.184, 555.186. Found: m/z = 553.117, 555.126. Crystal data [CCDC No. 961595]: $C_{20}H_{31}BClF_4IrN_4$ (**6**), M = 641.972, monoclinic, $P2_1/n$, a = 9.6053(10) Å, b = 17.4146(17) Å, c = 14.7645(15) Å, β = 102.613(3)°, V = 2410.1(4) Å^3, Z = 4, d_{calc} = 1.769 g/cm^3, T = 223 K, 24506 reflections collected, 5484 independent reflections (R_{int} = 0.0397), final R_1 = 0.0405, final wR_2 = 0.0834, GOF = 1.075.

*[(η^5-Pentamethylcyclopentadienyl)Ir^{III}bis-(κC-1,4-dimethyl-1,2,4-triazol-5-ylidene)Cl]BF$_4$ (**7**).* [Ag(TMe)$_2$]BF$_4$ was prepared as a colorless crystalline solid from [1,4-dimethyl-1,2,4-triazolium]BF$_4$, NaOH, and Ag_2O as described previously for imidazole-2-ylidenes.[25] [Cp*IrCl$_2$]$_2$ (80 mg, 0.1 mmol) and [Ag(TMe)$_2$]BF$_4$ (78 mg, 0.2 mmol) were dissolved in dry CH_2Cl_2 (5 mL), and the resulting orange suspension was stirred for 6 h at room temperature. The colorless precipitate was filtered off, the solution concentrated to ~2 mL under reduced pressure, and filtered again through a 0.2 μm pore size Teflon filter. The addition of Et_2O (10 mL) caused precipitation of a yellow-orange powder, which was collected and dried in vacuo. Yield = 113 mg (88%). ^{1}H NMR (400 MHz, CD_2Cl_2): δ = 8.22 (s, 2H, NC*H*N), 3.85 (s, 6H, NCH_3), 3.40 (s, 6H, NCH_3), 1.70 (s, 15H, $C_5(CH_3)_5$). ^{13}C{^{1}H}-NMR (125 MHz, CD_2Cl_2): δ = 151.4 (s, NCN), 145.7 (s, NCHN), 96.5 (s, $C_5(CH_3)_5$), 40.3 (s, NCH_3), 35.5 (s, NCH_3), 10.1 (s, $C_5(CH_3)_5$). ESI(+)MS calcd for $C_{18}H_{29}ClIrN_6^+$ (**7**-BF$_4$): 555.174, 557.177. Found: m/z = 555.411, 557.399. Crystal data [CCDC No. 961099]: $C_{20}H_{20}BClF_4IrN_6$ (**7**), M = 658.898, triclinic, $P\bar{1}$, a = 9.5222(17) Å, b = 10.0943(18) Å, c = 12.105(2) Å, α = 88.626(5)°, β = 81.821(5)°, γ = 87.868(5)°, V = 1150.7(4) Å^3, Z = 2, d_{calc} = 1.902 g/cm^3, T = 223 K, 11267 reflections collected, 4849 independent reflections (R_{int} = 0.0367), final R_1 = 0.0410, final wR_2 = 0.0710, GOF = 1.155.

*[(η^5-Pentamethylcyclopentadienyl)Ir^{III}bis-(κC-1,3-dimethylimidazol-2-ylidene)H]BF$_4$ (**6-H**).* **6** (128 mg, 0.2 mmol) and $NaBH_4$ (76 mg, 2 mmol) were placed in a flame-dried Schlenk flask under N_2 and dry isopropyl alcohol (10 mL) was added. The mixture was sonicated for 5 min and then stirred for another hour at room temperature. All volatiles were removed under reduced pressure to leave a beige solid, which was dried further in vacuo. The residue was extracted with CH_2Cl_2 (6 mL), the extract filtered through a 0.2 μm pore size Teflon filter, and the pale yellow solution was reduced to a volume of ~3 mL under reduced pressure. The addition of Et_2O (10 mL) caused precipitation of a very fine colorless solid, which was collected, washed with Et_2O (4 mL), and dried in vacuo. Yield = 110 mg (91%). ^{1}H NMR (500 MHz, CD_2Cl_2): δ = 7.02 (s, 4H, NC*H*C*H*N), 3.54 (s, 12 H, NCH_3), 1.93 (s, 15H, $C_5(CH_3)_5$), −16.24 (s, 1H, Ir*H*). ^{13}C{^{1}H}-NMR (125 MHz, CD_2Cl_2): δ = 149.9 (d, J = 5.2 Hz, NCN), 121.9 (s, NCHCHN), 92.8 (s, $C_5(CH_3)_5$), 39.1 (s, NCH_3), 10.5 (s, $C_5(CH_3)_5$). ESI(+)MS calcd for $C_{20}H_{32}IrN_4^+$ (**6**-**H**-BF$_4$): 519.223, 521.225. Found: m/z = 519.219, 521.223.

*[(η^5-Pentamethylcyclopentadienyl)Ir^{III}(κC,κC′-1,1′-methylene-bis-(3-methylimidazolidin-2-ylidene))H]BF$_4$ (**8-H**).* This compound has previously been obtained via a different synthetic route.[27] **8** (78 mg, 0.1 mmol) and $AgPF_6$ (26 mg, 0.11 mmol) placed in a flame-dried Schlenk flask under N_2 and MeCN added (3 mL). $NaBH_4$ (38 mg, 1 mmol) and isopropyl alcohol were then added, and the mixture stirred at 50 °C for 2 h. After cooling to room temperature, the mixture was filtered, and the pale yellow solution taken to dryness in vacuo. The solid residue was extracted with CH_2Cl_2 (4 mL) and filtered through a 0.2 μm pore size Teflon filter. The addition of Et_2O (12 mL) caused the precipitation of a pale yellow powder, which was collected, washed with Et_2O (3 mL), and dried in vacuo. Yield = 39 mg (60%). ^{1}H NMR (400 MHz, CD_2Cl_2): δ = 7.36 (d, J = 1.8 Hz, 2H, NC*H*CHN), 6.99 (d, J = 1.8 Hz, 2H, NCHC*H*N), 6.15 (d, J = 12.7 Hz, 1H, NCH_2N), 5.36 (d, J = 12.7 Hz, 1H, NCH_2N), 3.57 (s, 6H, NCH_3), 2.00 (s, 15H, $C_5(CH_3)_5$), −15.98 (s, 1H, Ir*H*).

Iridium(0) Nanoparticles. Ir NPs 2−3 nm in size were prepared using an adaption of a reported method.[48] [(coe)$_2$IrCl]$_2$ (9 mg, 0.01 mmol) in dry isopropyl alcohol (3 mL) was stirred under an atmosphere of H_2 at 60 °C until a grayish solution was obtained (15−30 min). At this point, the atmosphere was exchanged to N_2, and the solution was used directly for transfer hydrogenation catalysis.

Catalysis. All complexes used in catalysis were freshly purified prior to use. Complexes **8**[27] and **9**[62] were purified by recrystallization from chloroform at −78 °C, and complex **14**[30] was purified via column chromatography, as described in the original publications. All others

dx.doi.org/10.1021/cs400834q | ACS Catal. 2014, 4, 99−108

were purified by dissolution in a minimum amount of CH_2Cl_2, filtration through a hydrophobic 0.2 μm Teflon filter, and recrystallization via the addition of Et_2O, as described in the synthesis part. Catalytic runs were performed by charging a flame-dried Schlenk flask with 20 μmol Ir-complex and 0.2 mmol 1,3,5-trimethoxybenzene (TMB) as internal standard under N_2 and adding 2 mL dry isopropyl alcohol. After heating to the desired reaction temperature, liquid substrate (2 mmol acetophenone) and base (0.2 mmol KOH, semiconductor grade) were added in 1 mL of dry isopropyl alcohol to start the reaction. Aliquots were withdrawn by syringe and quenched by mixing with $CDCl_3$ in air at room temperature. After filtration through Celite, the solution was analyzed for conversion by ^{1}H NMR. In situ NMR reaction progress monitoring was performed in screw-capped 5 mm tubes, charged with solid iridium complex (0.007 mmol) and 1,3,5-trimethoxybenzene (0.067 mmol) under N_2. A solution of KOH (0.067 mmol) in dry isopropyl alcohol (1 mL) was added, followed by acetophenone (78 μL, 0.67 mmol). The NMR tube was sonicated for 30 s, placed in the NMR spectrometer with the probe preheated to 60 °C, and ^{1}H NMR spectra acquired every 2 min.

■ ASSOCIATED CONTENT

Supporting Information

Details of crystallographic analyses, CIF files, original NMR spectra of all compounds tested in catalysis, and variable-temperature NMR data. This material is available free of charge via the Internet at http://pubs.acs.org.

■ AUTHOR INFORMATION

Corresponding Authors

*E-mail: u.hintermair@bath.ac.uk (U.H.).
*E-mail: robert.crabtree@yale.edu (R.H.C.).

Present Addresses

[#]Department of Chemistry, University of Washington, Seattle, WA 98195, USA.
[‡]Division of Chemistry and Chemical Engineering, California Institute of Technology, Pasadena, CA 91125, USA.

Notes

The authors declare no competing financial interest.

■ ACKNOWLEDGMENTS

This material is based in part upon work supported by the Center for Catalytic Hydrocarbon Functionalization, an Energy Frontier Research Center funded by the U.S. Department of Energy, Office of Science, Office of Basic Energy Sciences (under Award No. DE-SC0001298 (R.H.C. and U.H. [synthesis]), by the U.S. Department of Energy, Office of Science, Office of Basic Energy Sciences catalysis (Award No. DE-FG02-84ER13297 (J.C. [kinetics] and N.D.S [structure]), and U.S. DoE Award 1043588 (T.P.B.). U.H. thanks the Alexander von Humboldt Foundation for a Feodor Lynen Research Fellowship, supplemented by a grant from the Yale Institute for Nanoscience and Quantum Engineering, and the Centre for Sustainable Chemical Technologies at the University of Bath for a Whorrod Research Fellowship. We thank Chris Incarvito (CBIC Yale) for help with X-ray crystallography and Mike Whittlesey (Bath) for valuable discussions.

■ REFERENCES

(1) Klomp, D.; Hanefeld, U.; Peters, J. A. In *The Handbook of Homogeneous Hydrogenation*; de Vries, J. G., Elsevier, C. J., Eds.; Wiley−VCH: Weinheim, Germany, 2007; Vol. 3, pp 585−630.
(2) Bullock, R. M. *Chem.—Eur. J.* **2004**, *10*, 2366−2374.
(3) Guillena, G.; Ramón, D. J.; Yus, M. *Angew. Chem., Int. Ed.* **2007**, *46*, 2358−2364.
(4) Nixon, T. D.; Whittlesey, M. K.; Williams, J. M. J. *Dalton Trans.* **2009**, 753−762.
(5) Dobereiner, G. E.; Crabtree, R. H. *Chem. Rev.* **2009**, *110*, 681−703.
(6) Watson, A. J. A.; Williams, J. M. J. *Science* **2010**, *329*, 635−636.
(7) Haddad, Y. M. Y.; Henbest, H. B.; Husbands, J.; Mitchell, T. R. B. *Proc. Chem. Soc.* **1964**, 361.
(8) Trocha-Grimshaw, J.; Henbest, H. B. *Chem. Commun.* **1967**, 544.
(9) Henbest, H. B.; Mitchell, T. R. B. *J. Chem. Soc. C* **1970**, 785−791.
(10) Camus, A.; Mestroni, G.; Zassinovich, G. *J. Mol. Catal.* **1979**, *6*, 231−233.
(11) Suzuki, T. *Chem. Rev.* **2011**, *111*, 1825−1845.
(12) Murata, K.; Ikariya, T.; Noyori, R. *J. Org. Chem.* **1999**, *64*, 2186−2187.
(13) Fujita, K.-i.; Yamaguchi, R. *Synlett* **2005**, *4*, 560−571.
(14) Zassinovich, G.; Mestroni, G.; Gladiali, S. *Chem. Rev.* **1992**, *92*, 1051−1069.
(15) Palmer, M. J.; Wills, M. *Tetrahedron: Asymmetry* **1999**, *10*, 2045−2061.
(16) Ikariya, T.; Blacker, A. J. *Acc. Chem. Res.* **2007**, *40*, 1300−1308.
(17) Saidi, O.; Williams, J. M. J. *Top. Organomet. Chem.* **2011**, *34*, 77−106.
(18) Hanasaka, F.; Fujita, K.-I.; Yamaguchi, R. *Organometallics* **2005**, *24*, 3422−3433.
(19) Corberán, R.; Peris, E. *Organometallics* **2008**, *27*, 1954−1958.
(20) Gnanamgari, D.; Sauer, E. L. O.; Schley, N. D.; Butler, C.; Incarvito, C. D.; Crabtree, R. H. *Organometallics* **2009**, *28*, 321−325.
(21) Berliner, M. A.; Dubant, S. P. P. A.; Makowski, T.; Ng, K.; Sitter, B.; Wager, C.; Zhang, Y. *Org. Process Res. Dev.* **2011**, *15*, 1052−1062.
(22) Pàmies, O.; Bäckvall, J.-E. *Chem.—Eur. J.* **2001**, *7*, 5052−5058.
(23) Samec, J. S. M.; Backvall, J.-E.; Andersson, P. G.; Brandt, P. *Chem. Soc. Rev.* **2006**, *35*, 237−248.
(24) Cp*Ir complexes bearing functional Noyori-type ligands have been investigated more thoroughly. See, for example: (a) Arita, S.; Koike, T.; Kayaki, Y.; Ikariya, T. *Organometallics* **2008**, *27*, 2795−2802. (b) Pannetier, N.; Sortais, J.-B.; Issenhut, J.-T.; Barloy, L.; Sirlin, C.; Holuigue, A.; Lefort, L.; Panella, L.; de Vries, J. G.; Pfeffer, M. *Adv. Synth. Catal.* **2011**, *353*, 2844−2852. (c) Cross, W. B.; Daly, C. G.; Boutadla, Y.; Singh, K. *Dalton Trans.* **2011**, *40*, 9722−9730. (d) O, W. W. N.; Lough, A. J.; Morris, R. H. *Organometallics* **2012**, *31*, 2152−2165.
(25) Hintermair, U.; Englert, U.; Leitner, W. *Organometallics* **2011**, *30*, 3726−3731.
(26) Xiao, X.-Q.; Jin, G.-X. *J. Organomet. Chem.* **2008**, *693*, 3363−3368.
(27) Vogt, M.; Pons, V.; Heinekey, D. M. *Organometallics* **2005**, *24*, 1832−1836.
(28) Ziessel, R. *J. Chem. Soc., Chem. Commun.* **1988**, 16−17.
(29) Li, L.; Brennessel, W. W.; Jones, W. D. *J. Am. Chem. Soc.* **2008**, *130*, 12414−12419.
(30) Brewster, T. P.; Blakemore, J. D.; Schley, N. D.; Incarvito, C. D.; Hazari, N.; Brudvig, G. W.; Crabtree, R. H. *Organometallics* **2011**, *30*, 965−973.
(31) Ziessel, R.; Youinou, M.-T.; Balegroune, F.; Grandjean, D. *J. Organomet. Chem.* **1992**, *441*, 143−154.
(32) Robertson, A.; Matsumoto, T.; Ogo, S. *Dalton Trans.* **2011**, *40*, 10304−10310.
(33) Polshettiwar, V.; Varma, R. S. *Green Chem.* **2009**, *11*, 1313−1316.
(34) Ouali, A.; Majoral, J.-P.; Caminade, A.-M.; Taillefer, M. *ChemCatChem* **2009**, *1*, 504−509.
(35) Miecznikowski, J. R.; Crabtree, R. H. *Organometallics* **2004**, *23*, 629−631.
(36) Allen, L. J.; Crabtree, R. H. *Green Chem.* **2010**, *12*, 1362−1364.
(37) Johnstone, R. A. W.; Wilby, A. H.; Entwistle, I. D. *Chem. Rev.* **1985**, *85*, 129−170.
(38) Hammond, C.; Schümperli, M. T.; Conrad, S.; Hermans, I. *ChemCatChem* **2013**, *5*, 2983−2990.

(39) Kantam, M. L.; Reddy, R. S.; Pal, U.; Sreedhar, B.; Bhargava, S. *Adv. Synth. Catal.* **2008**, *350*, 2231−2235.
(40) Alonso, F.; Riente, P.; Yus, M. *Tetrahedron Lett.* **2008**, *49*, 1939−1942.
(41) Verho, O.; Nagendiran, A.; Johnston, E. V.; Tai, C.-W.; Bäckvall, J.-E. *ChemCatChem* **2013**, *5*, 612−618.
(42) Alonso, F.; Riente, P.; Rodríguez-Reinoso, F.; Ruiz-Martínez, J.; Sepúlveda-Escribano, A.; Yus, M. *J. Catal.* **2008**, *260*, 113−118.
(43) Subramanian, T.; Pitchumani, K. *Catal. Sci. Technol.* **2012**, *2*, 296−300.
(44) Su, F.-Z.; He, L.; Ni, J.; Cao, Y.; He, H.-Y.; Fan, K.-N. *Chem. Commun.* **2008**, 3531−3533.
(45) Sonnenberg, J. F.; Coombs, N.; Dube, P. A.; Morris, R. H. *J. Am. Chem. Soc.* **2012**, *134*, 5893−5899.
(46) Toubiana, J.; Sasson, Y. *Catal. Sci. Technol.* **2012**, *2*, 1644−1653.
(47) Crabtree, R. H. *Chem. Rev.* **2012**, *112*, 1536−1554.
(48) Fonseca, G. S.; Scholten, J. D.; Dupont, J. *Synlett* **2004**, *2004*, 1525−1528.
(49) Foley, P.; DiCosimo, R.; Whitesides, G. M. *J. Am. Chem. Soc.* **1980**, *102*, 6713−6725.
(50) Widegren, J. A.; Finke, R. G. *J. Mol. Catal. A: Chem.* **2003**, *198*, 317−341.
(51) Dröge, T.; Glorius, F. *Angew. Chem., Int. Ed.* **2010**, *49*, 6940−6952.
(52) As we observed the formation of a colorless precipitate under reaction conditions, we suspect a solubility limitation of the active species to cause the observed saturation. Unfortunately, these in-situ-formed solids eluded characterization as they quickly changed color upon attempted isolation.
(53) Gilbert, T. M.; Bergman, R. G. *J. Am. Chem. Soc.* **1985**, *107*, 3502−3507.
(54) Glueck, D. S.; Winslow, L. J. N.; Bergman, R. G. *Organometallics* **1991**, *10*, 1462−1479.
(55) Pons, V.; Heinekey, D. M. *J. Am. Chem. Soc.* **2003**, *125*, 8428−8429.
(56) Campos, J.; López-Serrano, J.; Álvarez, E.; Carmona, E. *J. Am. Chem. Soc.* **2012**, *134*, 7165−7175.
(57) Abura, T.; Ogo, S.; Watanabe, Y.; Fukuzumi, S. *J. Am. Chem. Soc.* **2003**, *125*, 4149−4154.
(58) Hu, Y.; Li, L.; Shaw, A. P.; Norton, J. R.; Sattler, W.; Rong, Y. *Organometallics* **2012**, *31*, 5058−5064.
(59) Furthermore, the test assumes that active monohydride intermediates do not engage in exchange mechanisms.
(60) Wilkes, J. S.; Zaworotko, M. J. *J. Chem. Soc., Chem. Commun.* **1992**, 965−967.
(61) Ball, R. G.; Graham, W. A. G.; Heinekey, D. M.; Hoyano, J. K.; McMaster, A. D.; Mattson, B. M.; Michel, S. T. *Inorg. Chem.* **1990**, *29*, 2023−2025.
(62) Parent, A. R.; Brewster, T. P.; De Wolf, W.; Crabtree, R. H.; Brudvig, G. W. *Inorg. Chem.* **2012**, *51*, 6147−6152.